



Classifying California plant species temporally using airborne hyperspectral imagery

Susan K. Meerdink^{a,b,*}, Dar A. Roberts^a, Keely L. Roth^c, Jennifer Y. King^a, Paul D. Gader^b, Alexander Koltunov^d

^a Department of Geography, University of California Santa Barbara, Santa Barbara, CA 93106-4060, United States

^b Engineering School of Sustainable Infrastructure and Environment, University of Florida, Gainesville, FL 32611, United States

^c The Climate Corporation, San Francisco, CA 94103, United States

^d University of California Davis, Center for Spatial Technologies and Remote Sensing (CSTARS), Department of Land, Air, and Water Resources, United States



ARTICLE INFO

Edited by Emilio Chuvieco

Keywords:

Plant species classification
Hyperspectral
Imaging spectroscopy
HyspIRI
AVIRIS
Discriminant analysis
Time series
Vegetation phenology

ABSTRACT

Accurate knowledge of seasonal and inter-annual distributions of plant species is required for many research and management agendas that track ecosystem health. Airborne imaging spectroscopy data have been used successfully to map plant species, but often only in a single season or over a limited spatial extent due to data availability. NASA's Hyperspectral Infrared Imager (HyspIRI) preparatory airborne campaign flew an imaging spectrometer from 2013 to 2015. This dataset captured a severe drought and thus provided the opportunity to evaluate species discrimination over an extreme range in environmental conditions. Here we evaluate the portability of image-based training data and accuracy of species discrimination. The imagery was acquired in the spring, summer, and fall seasons of 2013–2015 with the Airborne Visible/Infrared Imaging Spectrometer (AVIRIS). Reference spectral libraries were developed with three sets of spectra: spectra from a single image date, combining spectra from multiple dates (by season, by year, and from all dates), and creating leave-one-out (LOO) libraries that pooled spectra from all dates but one. Canonical discriminant analysis (CDA) was applied to reduce data dimensionality, and classification was performed using linear discriminant analysis (LDA). When only spectra from the same image date were used, plant species were classified with a mean kappa accuracy ranging between 0.80 and 0.86 for the nine dates. Seasonal and annual spectral libraries had comparable accuracies with mean kappa 0.79–0.83 and 0.78–0.83, respectively. Seasonal libraries performed slightly better than annual libraries for species because they better-incorporated changes in spectra due to phenology. Spectral libraries were not transferable across dates, with mean kappa accuracies dropping to 0.31–0.73 for LOO spectral libraries. These results emphasize that spectral libraries built from previously collected imagery may not be able to map plant species over new images accurately. Specifically, our results highlight the need to use reference spectra that adequately represent the phenological and biophysical status of the plant species within an image for accurate mapping. Our research provides relevant insight for advanced species-mapping techniques across broad spatial and temporal scales using imagery from sensors like HyspIRI.

1. Introduction

Plant species maps provide a baseline for monitoring the world's ecosystems, which are already responding to climate change (Walther et al., 2002). Globally, researchers have documented shifts in plant phenology that provide compelling evidence of species being influenced by environmental change (Cleland et al., 2007). For example, in Southern California, increasing air temperature and decreasing precipitation have already caused distribution shifts in ten widely distributed plant species (Kelly and Goulden, 2008). In order to quantify

these changes, plant species maps are crucial for many applications, including monitoring invasive species expansion (Underwood et al., 2003), tracking wildfire disturbance recovery (Riaño et al., 2002), and detecting vegetation disturbances such as insect infestation (Lawrence and Labus, 2003; Tane et al., 2018a).

There are many techniques for developing species maps, including ground-based approaches, but remote sensing technology allows for the investigation of ecological processes and systems on larger spatial and temporal scales. Imaging spectroscopy, or hyperspectral remote sensing, makes discrimination of plant species possible because the

* Corresponding author.

E-mail address: susanmeerdink@ufl.edu (S.K. Meerdink).

hundreds of narrow bands can be used to detect subtle spectral shifts between species that are caused by differences in chemistry, physiology, and structure (Asner and Martin, 2008; Roberts et al., 2004). Using sensors such as the airborne visible/infrared imaging spectrometer (AVIRIS) or HYperspectral Digital Imagery Collection Experiment (HYDICE) sensor, plant species in diverse ecosystems have been classified successfully (Clark et al., 2005; Martin et al., 1998; Roth et al., 2015a; van Aardt and Wynne, 2007). While these studies demonstrate the ability to classify plant species, past research has been temporally restricted to a single image date.

Very few studies have addressed these temporal limitations due to the availability of airborne hyperspectral imagery. However, to capture ecosystem changes over time, it is necessary to develop remote sensing techniques that incorporate a plant's annual and seasonal variability. A plant's spectral response changes throughout the year due to phenology, such as timing of leaf, flowering, and stem elongation events (Gill and Mahall, 1986; Vina et al., 2004). Classification rules developed for a given date may not apply to other dates due to changes in species' spectral response throughout the season and from year to year (Peñuelas and Filella, 1998). In regional studies, seasonal and inter-annual changes in plant spectra have been shown to be important for separating plant species during a drought and from invasive species (Burkholder et al., 2011; Dennison et al., 2003). Additionally, some species (e.g., annual vs. perennial, deciduous vs. evergreen) have distinct phenology compared to other species that could improve classification accuracy (Gill and Mahall, 1986; Hufstader, 1978). Dudley et al. (2015) incorporated a single year's phenology into species classifications and found that multi-temporal spectral libraries achieved similar overall classification accuracy compared to single-date libraries. However, Dudley et al. (2015) were restricted to a single year and a small geographic area which does not address the ability to classify species over multiple years. With increasing amounts of hyperspectral data available, the use of temporally transferrable training data could reduce analysis and processing time involved in plant species classification.

Plant species mapping research has been restricted to airborne platforms because current space-borne systems cannot generate the level of spectral detail needed to discriminate between species (Cohen and Goward, 2004; Ustin et al., 2004). One exception is the space-borne Hyperion mission (e.g., George et al., 2014; Koedsin and Vaiphasa, 2013; Somers and Asner, 2013), but this mission was a sampling mission and deactivated in March 2017. Promising new sensor systems, such as the proposed Hyperspectral Infrared Imager (HyspIRI) mission, would be able to quantify the plant species distributions and physiological functions required to address this need (Lee et al., 2015). The HyspIRI mission would provide hyperspectral imagery with global coverage of Earth's ecosystems every 16 days, at 30 m spatial resolution, resulting in a significantly larger dataset with which to develop species maps through time. While the need for this instrumentation was identified in the 2017 decadal survey, no launch date has been announced (National Academies of Sciences and Medicine, 2018).

To develop precursor datasets in advance of the HyspIRI mission, the National Aeronautics and Space Administration (NASA) flew airborne instruments starting in 2013. The goal of this three-year campaign was to demonstrate the range of critical scientific applications that can be uniquely addressed with the HyspIRI mission (Lee et al., 2015). Flying over large swaths of California and capturing the worst drought on record for the state, this campaign has been leveraged by multiple studies (Bell et al., 2015; Coates et al., 2015; He et al., 2015; Palacios et al., 2015; Tane et al., 2018b; Wang et al., 2015; Wetherley et al., 2017).

Our study leverages this unique dataset collected during the HyspIRI airborne preparatory campaign to explore the capabilities of seasonal and annual plant species classification. Collecting reference spectra is time-consuming and expensive, especially for ecosystems with rugged terrain. Ideally, for efficient processing of future datasets,

spectral libraries would incorporate temporal variability to maintain accuracy when applied to newly collected imagery or locations. Traditionally, classification efforts take care to include spectral data from a similar climatic regime or timeframe, but we test whether these constraints can be loosened while retaining classification accuracy. Our study determines and quantifies the extent to which plants' temporal spectra can be used to generate accurate plant species classification maps. To establish baseline classification capabilities, we developed spectral libraries from a single image date to classify 27 plant species and land cover classes. We then combined seasonal and annual spectra to evaluate our ability to map plant species with increased seasonal or annual spectral variability. Finally, we used leave-one-out (LOO) libraries that pooled spectra from all but one date to determine how transferable libraries are across image dates. Our overarching objective is to determine how effectively spectra collected from seasonal or annual imagery can be used to classify species over multiple years and across a large landscape—nearly 13,000 km². Specifically, we asked the following questions:

1. How accurately can California plant species be classified using imagery from 2013 to 2015 spring, summer, and fall?
2. Can a multiple date spectral library be used to map species annually and seasonally?
3. How transferable are spectral libraries across dates for species classifications?

2. Methods

2.1. Study site and image acquisition

The imagery was collected with the AVIRIS sensor as part of the HyspIRI Airborne Preparatory Campaign. AVIRIS measures 224 bands of radiance between 360 and 2500 nm with a full width at half-maximum of 10 nm (Green et al., 1998). The sensor was flown on the NASA ER-2 aircraft at an altitude of 20 km over six flight boxes in California to simulate future satellite imagery from HyspIRI (Lee et al., 2015). This study uses a spatial subset of imagery from the Santa Barbara flight box, which includes ten of the eleven flight lines that were acquired with a 35° northeast-southwest orientation (Fig. 1). These ten flight lines cover a diverse landscape that is approximately 12,980 km². The majority of this area falls into the Los Padres National Forest (LPNF), while the remainder is privately owned land or urbanized. The elevation increases from sea level to a peak of 2697 m with the imagery capturing the transition from chaparral shrubland to conifer forests located in the LPNF. The entire study area experiences a Mediterranean climate characterized by wet, cool winters and dry, hot summers. Annual precipitation for the area ranges from 250 to 1000 mm with 95% falling between November and March (Davis and Michaelsen, 1995; Diamond et al., 2013). However, during the time period studied (2013–2015), this area experienced an extreme drought (Griffin and Anchukaitis, 2014; Swain et al., 2014). The campaign flew three times per year, thus capturing April, June, and November or August imagery during 2013, 2014, and 2015 (Table 1). Two flight lines were excluded, and two were replaced with another date due to technical errors when collecting the data, resulting in 88 AVIRIS images used in our analysis.

2.2. Image processing

NASA's Jet Propulsion Laboratory (JPL) provided 18 m spatial resolution reflectance products simulated using AVIRIS imagery (Thompson et al., 2015). To use the AVIRIS dataset across flight dates, a series of additional preprocessing steps were required. The custom source code developed for this study and used to process AVIRIS imagery is available at <https://github.com/susanmeerdink/AVIRIS-Image-Preprocessing>. The preprocessing steps, described below, can be summarized as registration across dates, geolocation refinement, and

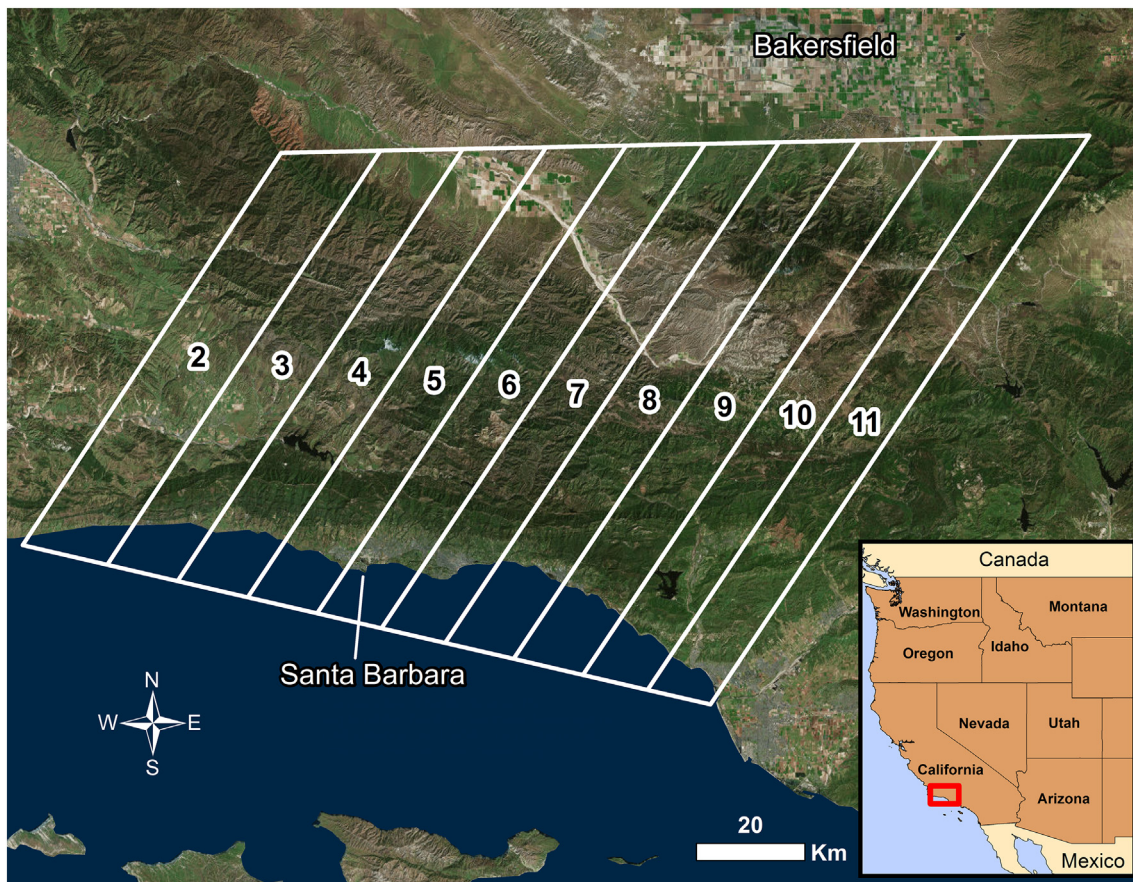


Fig. 1. Santa Barbara flight box and the HypsIPI Airborne Preparatory campaign flight lines used in the study.

relative radiometric normalization. Image processing was completed using ENVI+IDL software (Exelis Visual Information Solutions, Boulder, CO, USA).

Although initially geolocated by the JPL, the AVIRIS images exhibited significant systematic spatial misalignment on the scale of multiple pixels. Therefore, the first preprocessing step registered the images across dates to approach a subpixel level alignment required for multi-date studies. Because using manually selected control points rarely delivers subpixel accuracy, and due to the large number of images needing to be registered, we applied an automated registration algorithm (Koltunov et al., 2012). This algorithm has been successfully used in previous multi-temporal AVIRIS studies involving spectral unmixing (e.g., Khanna et al., 2017, 2013; Tane et al., 2018a) and other change detection research (Koltunov et al., 2016, 2009). This algorithm represents band-wise iterations of relative radiometric normalization between the reference and the source images, followed by a gradient-based video-sequence stabilization method (Irani, 2002) that estimates the unknown parameters of a chosen between-image motion model.

Each image was visually inspected to determine the band and model (affine or shift) that resulted in the best registration. The 16 Apr 2014 flight lines were selected as the reference images for registration of all other dates because all ten flight lines were available for that date and no cloud cover was present.

During the second step, the registered images were georeferenced to correct absolute georeferencing error. The National Agriculture Imagery Program (NAIP) digital orthophotos acquired in the spring and fall of 2012 were utilized as a base map for this process. The orthophotos were mosaicked and resampled to 18 m spatial resolution and then used to collect ground control points for the 16 Apr 2014 flight lines. Because all images were co-registered in the previous step, the image coordinates for the control points on 16 Apr 2014 flight lines were applied for all other image dates.

The final processing step was a relative radiometric normalization of the image products. During 2013–2015, the HypsIPI simulated reflectance product was actively in development, which made it challenging to compare spectra across flight dates. To compensate for

Table 1

Dates and flight lines covered for the Santa Barbara flight box. The * symbol denotes deviations from other flight line dates.

		FL02	FL03	FL04	FL05	FL06	FL07	FL08	FL09	FL10	FL11
2013	Spring	04/11/13	04/11/13	04/11/13	04/11/13	04/11/13	04/11/13	04/11/13	04/11/13	04/11/13	04/11/13
2013	Summer	06/06/13	06/06/13	06/06/13	06/06/13	06/06/13	06/06/13	06/06/13	06/06/13	06/06/13	06/06/13
2013	Fall	11/25/13	11/25/13	11/25/13	N/A	11/25/13	11/25/13	11/25/13	11/25/13	11/25/13	11/25/13
2014	Spring	04/16/14	04/16/14	04/16/14	04/16/14	04/16/14	04/16/14	04/16/14	04/16/14	04/16/14	04/16/14
2014	Summer	06/06/14	06/06/14	06/06/14	06/06/14	N/A	06/04/14*	06/06/14	06/06/14	06/04/14*	06/06/14
2014	Fall	08/29/14	08/29/14	08/29/14	08/29/14	08/29/14	08/29/14	08/29/14	08/29/14	08/29/14	08/29/14
2015	Spring	04/16/15	04/16/15	04/16/15	04/16/15	04/16/15	04/16/15	04/16/15	04/16/15	04/16/15	04/16/15
2015	Summer	06/02/15	06/02/15	06/02/15	06/02/15	06/02/15	06/02/15	06/02/15	06/02/15	06/02/15	06/02/15
2015	Fall	08/24/15	08/24/15	08/24/15	08/24/15	08/24/15	08/24/15	08/24/15	08/24/15	08/24/15	08/24/15

atmospheric artifacts and noise, a linear correction was developed for each date and applied to the corresponding images (Clark et al., 2002; Wetherley et al., 2018). The correction was developed by creating a band-by-band ratio of reflectance values using an invariant target's field and image spectra (Fig. S1). The roof of the United States Postal Service distribution center in Goleta, CA, was selected as the invariant target (Thompson et al., 2015). On 2 May 2014, spectra were collected on the roof using an Analytical Spectra Device Full Range spectrometer which covers the 0.3–2.5 μm range with a sampling interval of 1 nm (Analytical Spectral Devices, Inc., Boulder, CO USA). Image spectra were collected from 15 to 20 pixels for each of the nine image dates. The invariant target fell on flight line 5 or 6, depending on the flight date. This approach assumes that ground targets are temporally invariant and reflectance retrieval errors are systematic for all flight lines acquired on the same date.

2.3. Reference data

Reference data on the spatial distribution of dominant species and land cover types were collected both in the field and using AVIRIS and NAIP imagery. In the field, we used a composition estimation method where patches of dominant plant species and their relative composition were collected using a high-power spotting scope and laser range finder from remote vantage points (Meentemeyer et al., 2001). Vantage points for the spotting scope were selected based on accessibility through hiking or driving. The patches ranged in size from 1296 m² to 249,804 m². Patches having > 75% single species composition were recorded and digitized on the AVIRIS flight line. These patches were stored with location and metadata as polygons in a shapefile. Species that were consistently found growing in mixed patches were treated as a single class (e.g., ARCA-SALE and ATCA-ERNA, Table 2). In this study, 700 reference polygons were collected to cover new species and locations not previously covered in other studies. These polygons were in addition to approximately 400 polygons collected previously (Roberts et al., 2015; Roth et al., 2015a). Reference polygons were used to extract spectra from imagery, and only pixels completely falling into a reference polygon were used to develop spectral libraries. The species

codes, the total number of polygons, and pixels for each class are shown in Table 2

2.4. Spectral library development, dimensionality reduction, and classification

As mentioned previously, this study area was undergoing a severe drought when images were captured. Drought has a direct effect on the timing of plant phenological events. The periods of greenup, maturity, senescence, and dormancy were identified from the Moderate Resolution Imaging Spectroradiometer (MODIS) Land Cover Dynamics (MCD12Q2) Version 6 data product (Fig. 2; Zhang et al., 2006). This algorithm characterizes vegetation growth cycles using four transition dates estimated from time series of MODIS Enhanced Vegetation index (EVI) data: (1) green-up: the date of onset of EVI increase; (2) maturity: the date of onset of EVI maximum; (3) senescence: the date of onset of EVI decrease; and (4) dormancy: the date of onset of EVI minimum (Verma et al., 2010; Zhang et al., 2006, 2003). At the peak of the drought in 2014, the median date for green-up and maturity occurred later in the year compared to 2013 and 2015. The majority of agricultural regions were excluded, but some outliers in green-up and senescence are the result of some farms that were not excluded. Due to the size of the study area (~13,000 km²), there was large variability in start dates, resulting in significant overlap of phenology stages. Plants near the coast had early green-up dates compared to plants further inland, especially for those on the leeward side of the mountains. Phenological events will differ between species and environmental conditions, making it difficult to separate at a landscape scale. Ideally, temporal division of spectral libraries would occur with the corresponding phenological stage. However, we temporally divided spectral libraries according to calendar dates instead of phenology because only nine dates were available, and the size of the study area created large variability. Future work should focus on developing spectral libraries or methodologies that appropriately divide samples spatially and temporally for a particular study area.

Altogether, 25 spectral libraries were developed and used to classify the nine image dates (Table 3). There were three categories of spectral libraries: single date, multiple date, and leave-one-out (LOO). Nine single date libraries, which only included spectra from each respective image date, were developed. There were seven multiple date spectral libraries in which three were developed from seasonal images, three were developed from yearly images, and one was developed from all images. The seasonal spectral libraries had spectra from a season across the three years of image dates (e.g., Spr-All, Sum-All, Fall-All). The yearly spectral libraries also had spectra from three image dates that were restricted to a single year (e.g., 2013-All, 2014-All, 2015-All). The last multiple date library was the All-Dates library developed using all nine image dates. The final spectral library category, leave-one-out (LOO) cross-validation spectral libraries, tested whether spectra from all other dates could accurately classify an image. In these libraries, one date was left out from the spectral library. Table 3 specifies which image dates were used in the development of each spectral library. Development of spectral libraries, classification, and statistics were performed using MATLAB (The Mathworks Inc., Natick, MA, USA). Significance testing across classification results was performed using One-way Analysis of Variance (ANOVA) with the Dunn-Sidak adjustment. Significance testing shown in Figs. S11–S14 was performed using t-tests comparing an individual species user or producer accuracy between single date classification and one other classification (seasonal, yearly, or all dates).

For each spectral library, data were randomly split into training and validation sets over 50 iterations (Fig. 3). For each iteration, 70% of a species' reference polygons were randomly selected for training, while the remaining 30% were used for validation. Because polygon sizes differ, a maximum of ten pixels were randomly selected from each polygon until the total number of training pixels reached 350 for each

Table 2
Dominant classes mapped with corresponding abbreviations, polygon, and pixel counts.

Species	Code	Polygons	Pixels
<i>Adenostoma fasciculatum</i>	ADFA	75	2063
Agricultural Residue	AGRES	59	1359
<i>Artemisia californica</i> and <i>Salvia leucophylla</i>	ARCA-SALE	61	1702
<i>Arctostaphylos</i> spp.	ARGL	53	1276
<i>Atriplex canescens</i> and <i>Ericameria nauseosa</i>	ATCA-ERNA	36	659
<i>Baccharis pilularis</i>	BAPI	19	323
<i>Brassica nigra</i>	BRNI	47	1357
<i>Ceanothus cuneatus</i>	CECU	24	462
<i>Ceanothus megacarpus</i>	CEME	55	1544
<i>Ceanothus spinosus</i>	CESP	31	867
<i>Citrus</i> spp.	CISP	30	628
<i>Eriogonum fasciculatum</i>	ERFA	30	989
<i>Eucalyptus</i> spp.	EUSP	44	1257
Irrigated Grasses	IRGR	35	538
<i>Juniperus californica</i>	JUCA	15	178
Mediterranean Annual Grasses and Forbs	MAGF	58	3075
<i>Persea Americana</i>	PEAM	60	2187
<i>Pinus jeffreyi</i>	PIJE	16	226
<i>Pinus monophylla</i>	PIMO	36	531
<i>Pinus sabiniana</i>	PISA	34	854
<i>Pseudotsuga menziesii</i>	PSMA	11	261
<i>Quercus agrifolia</i>	QUAG	42	1152
<i>Quercus berberidifolia</i>	QUBE	36	426
<i>Quercus douglasii</i>	QUDO	37	1115
Rock	ROCK	26	463
Soil	SOIL	40	835
<i>Umbellularia californica</i>	UMCA	27	817

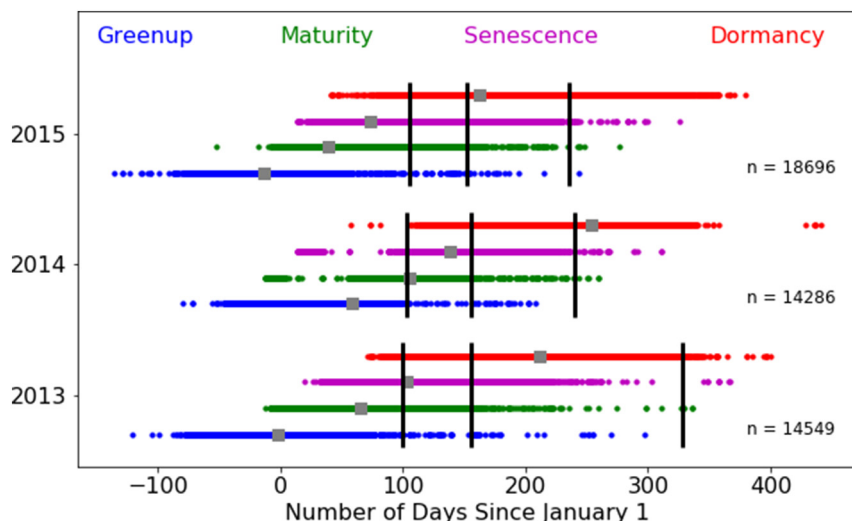


Fig. 2. 2013–2015 key phenology dates for all pixels in the study area measured from the Moderate Resolution Imaging Spectroradiometer (MODIS) Land Cover Dynamics (MCD12Q2) Version 6 data product. Gray squares show median date, and black lines show dates when images were captured.

Table 3

Spectra from image dates used to develop spectral libraries. Note that fall 2013 imagery was collected in November, while 2014 and 2015 fall dates were collected in August.

	Library Name	Spectra from Image Dates		
Single-Date Libraries	Spr-2013	04/11/2013		
	Sum-2013	06/06/2013		
	Fall-2013	11/25/2013		
	Spr-2014	04/16/2014		
	Sum-2014	06/06/2014		
	Fall-2014	08/29/2014		
	Spr-2015	04/16/2015		
	Sum-2015	06/02/2015		
	Fall-2015	08/24/2015		
Multiple Date Libraries	Spr-All	04/11/2013	04/16/2014	04/16/2015
	Sum-All	06/06/2013	06/06/2014	06/02/2015
	Fall-All	11/25/2013	08/29/2014	08/24/2015
	2013-All	04/11/2013	06/06/2013	11/25/2013
	2014-All	04/16/2014	06/06/2014	08/29/2014
	2015-All	04/16/2015	06/02/2015	08/24/2015
	All-Dates	All nine image dates		
Leave-One-Out (LOO) Libraries	LOO-Spr13	All dates except 04/11/2013		
	LOO-Sum13	All dates except 06/06/2013		
	LOO-Fall13	All dates except 11/25/2013		
	LOO-Spr14	All dates except 04/16/2014		
	LOO-Sum14	All dates except 06/06/2014		
	LOO-Fall14	All dates except 08/29/2014		
	LOO-Spr15	All dates except 04/16/2015		
	LOO-Sum15	All dates except 06/02/2015		
	LOO-Fall15	All dates except 08/24/2015		

species. This was implemented to create a balanced training dataset because not all species had the same number of polygons or pixels (Table 2). The threshold was selected based on previous work (Roth et al., 2012). If a polygon fell on two flight lines, spectra from both flight lines were included. The multiple date and LOO libraries used the same training pixels as the single dates. This resulted in each date having an even number of spectra and larger libraries compared to single date libraries.

Each spectral library underwent dimensionality reduction using canonical discriminant analysis (CDA), a technique which was previously found to achieve the best species-level separation for a library

```

FOR each iteration
  FOR each species
    Randomly select 70% of polygons for training
    Set remaining 30% of polygons for validation
    Set number of training pixels to 0
    FOR each polygon selected for training
      IF polygon has more than 10 pixels
        Randomly select 10 pixels in polygon
      ELSE
        Select all pixels in polygon
      END
      Add indices and number of training pixels selected
      IF training pixel count is greater than 350
        Continue onto next species
    END
  END
END

```

Fig. 3. Pseudocode describing the process of splitting reference polygons into training and validation. Training and validation libraries were used to calculate the Canonical Discriminant Analysis (CDA) and perform accuracy assessment on Linear Discriminant Analysis (LDA) classification.

(Alonso et al., 2013; Roth et al., 2015b, 2015a). CDA reduces the data by finding orthogonal components while deriving functions which maximize linear separation among groups (e.g., plant species; Klecka, 1980). The number of functions derived is equal to the number of groups minus one. CDA coefficients were calculated for the 50 iterations of training pixels. These 50 coefficients were averaged and applied to the training and validation spectra for dimensionality reduction (Cruz-Castillo et al., 1994). CDA coefficients were average to reduce the processing time on classification of imagery instead of running 50 iterations over the 88 AVIRIS images.

Linear discriminant analysis (LDA) was run using CDA-transformed spectra to classify plant species. LDA derives linear combinations of the canonical variables which best correlate with class membership (Fisher, 1936). LDA was trained using the same training pixels selected in the 50 iterations to develop CDA coefficients. When LDA was applied to the validation polygons, the polygon class was determined by the pixel majority. If the class matched the validation polygon plant identification, the polygon classification was considered correct. Class separability was evaluated using the kappa coefficient (Congalton, 1991),

Table 4

Average classification kappa accuracy for each image date using single date spectral libraries. Averaged kappa accuracy is calculated from 50 iterations. Bold designates spectral libraries that contain image date spectra. Rows report the spectral library, while columns report image dates.

	Image date								
	Spr 2013	Sum 2013	Fall 2013	Spr 2014	Sum 2014	Fall 2014	Spr 2015	Sum 2015	Fall 2015
Spr-2013	0.85	0.41	0.26	0.42	0.13	0.21	0.29	0.26	0.22
Sum-2013	0.35	0.84	0.26	0.36	0.25	0.37	0.34	0.37	0.37
Fall-2013	0.24	0.18	0.80	0.19	0.12	0.30	0.27	0.28	0.32
Spr-2014	0.06	0.07	0.19	0.84	0.20	0.36	0.39	0.43	0.34
Sum-2014	0.14	0.22	0.14	0.22	0.85	0.29	0.38	0.19	0.26
Fall-2014	0.01	0.06	0.10	0.40	0.13	0.85	0.41	0.48	0.54
Spr-2015	0.03	0.03	0.09	0.35	0.14	0.29	0.83	0.29	0.29
Sum-2015	0.09	0.13	0.19	0.36	0.18	0.29	0.34	0.86	0.38
Fall-2015	0.04	0.09	0.09	0.32	0.19	0.35	0.33	0.35	0.85

overall accuracy, and class-level producer's and user's accuracies. The kappa coefficients between classifications were evaluated for statistical significance using one-way ANOVA with the Dunn-Sidak adjustment in MATLAB. All 225 classifications with overall and kappa accuracy can be found in Tables S1–S3.

3. Results

3.1. Single date spectral libraries

Spectral libraries developed from a single image date were used to develop baseline capabilities for classifying the plant species in this study (Table 4). Overall, the 27 plant species and land cover classes in this study were successfully classified with high accuracies across dates and diverse ecosystems using single date spectral libraries. Single date spectral libraries classifying the corresponding image date, such as the Spr-2013 library applied to the Spring 2013 imagery, resulted in the highest classification accuracies, ranging from 0.80 to 0.86 kappa across the nine image dates. Single date libraries used to classify an unrelated image, such as the Spr-2013 library applied to the Summer 2013 imagery, performed poorly with all kappa accuracies below 0.5. Species spectra distributions were significantly different between image dates, which produced lower accuracies when classifying an image with a spectral library from a different date.

For single date image classification, accuracies were not consistent across seasons or years (Fig. 4). The 2013 and 2014 spring imagery had

the highest classification accuracy (kappa mean of 0.84). These two image dates captured new seasonal leaf growth for many of the species studied. The image classification of 2013 spring imagery shows the expected plant species distributions with conifer forests found northeast in the Los Padres National Forest and the southern edge containing the chaparral communities traditionally found in this region (Fig. 5). The 2013 fall imagery had the lowest accuracy, but only marginally with a kappa mean of 0.80. However, the classification errors are visually apparent in the image compared to other dates, with conifers (PSMA and PIJE) having much lower accuracies (Fig. 5). Classification of 2013 Fall imagery was difficult for two reasons: plants were fully senescent which reduces spectral separability, and the imagery was collected particularly late in the year (November) causing lighting geometry to impact the plant species classification adversely. The 2014 summer image deviated the most from expected plant species distributions despite having high accuracies with library classification (Fig. 5). Flight line 2 (extreme western flight line) had the most pronounced cross track variation due to bidirectional reflectance distribution function (BRDF) effects. These effects are also present in other images, but less so due to a collection time closer to solar noon. Zoomed in portions of the classification show how predicted distributions shift across images dates (Fig. 6; Fig. 7). The other image date classifications can be found in Figs. S2–S10.

The user and producer's accuracies for individual species show marked differences between species and dates (Fig. 8; Figs. S11–S14). Classification accuracy was not consistent across seasons and years for

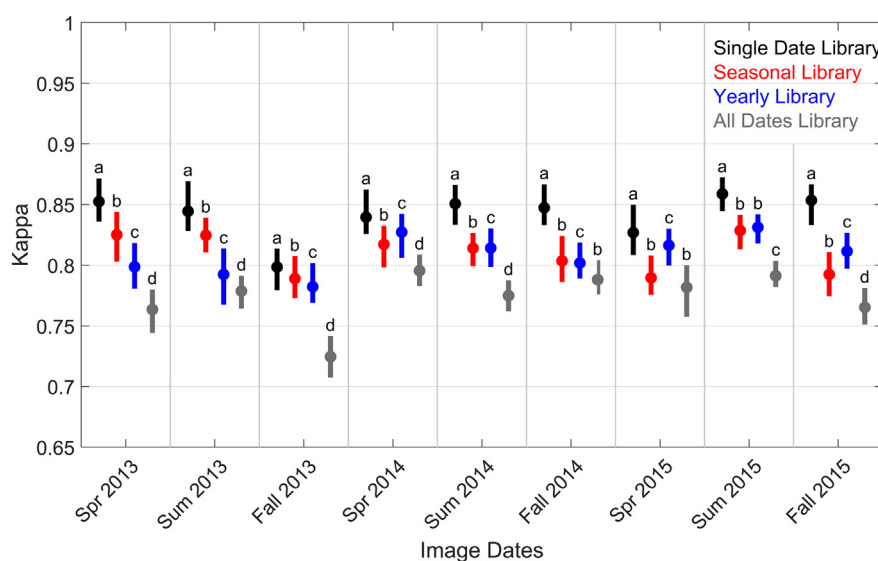


Fig. 4. Classification accuracy of all nine images using four different spectral libraries. Dots represent mean classification accuracy with the top and bottom of bars marking the maximum and minimum accuracies. Letters designate libraries that are significantly different for each date ($p < 0.05$).

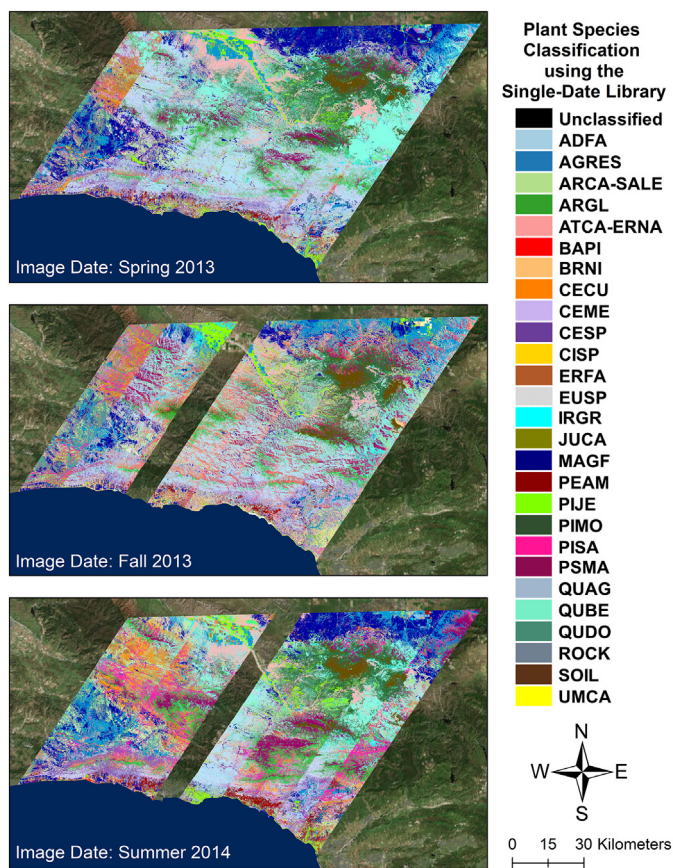


Fig. 5. Plant species classification of Spring 2013, Fall 2013, and Summer 2014 imagery using the corresponding single date spectral library. Other image classifications can be found in Figs. S2–S10.

species with overall low accuracies, while species with high accuracies resulted in little variation across dates (Fig. 9). For example, the seasonal differences and range of accuracies for JUCA and PIMO (the two species with the lowest accuracies) are more substantial than for QUDO and ARCA-SALE (the two species with the highest accuracies). These four species and species-combinations illustrate how canopy geometry and morphology influence species' classification accuracies. While common on the landscape, JUCA grows dispersed with, at times, meters of bare substrate or grass between individuals. Evergreen trees, such as PIMO, have sparse canopies and therefore tend to have spectra that are highly influenced by the substrate. On the other hand, ARCA-SALE form dense canopies with limited influence of the substrate on the spectra. QUDO is a broadleaf tree with canopies larger than the 18 m spatial resolution, so no other species influence pixel spectra. Species that tend to grow interspersed with other species, such as ARGL, also have lower accuracies and are often confused by the classifier with their respective interspersed species, such as ADFA.

3.2. Multiple date spectral libraries

In order to test our capability of classifying plant species across a time series, multiple-date spectral libraries were developed (Table 5). Image dates were classified satisfactorily if the spectral library contained spectra from that specific image date. For example, the Spring 2013 imagery was classified accurately with the Spr-All (0.83 mean kappa) and 2013-All (0.80 mean kappa) spectral libraries but had low accuracies with Fall-All (0.20 mean kappa) and 2015-All (0.09 mean kappa) spectral libraries. Seasonal and yearly differences in spectra made classification difficult when using spectral libraries derived exclusively from other image dates.

For all image dates, the single date spectral library outperformed all non-inclusive multiple date libraries (Fig. 4). However, the corresponding seasonal or yearly libraries were comparable to single-date kappa values. The inclusion of other seasonal and annual spectra dropped the accuracy by 0.01–0.06 kappa compared to single-date classification's kappa. In general, the season-based spectral libraries (0.79–0.83 mean kappa) performed similarly to year-based spectral libraries (0.78–0.83 mean kappa). The spectral library containing all image dates, performed consistently low across all nine dates. The inclusion of spectra from all nine dates with the All-Dates library dropped classification accuracy by 0.03–0.10 kappa compared to the single date library. However, it is worth noting for Fall 2014 and Spring 2015 imagery, the performance of the All-Dates spectral library was not significantly different from that of the seasonal library.

Producer and user's accuracies for individual species also decreased with the use of multiple-date spectral libraries (Fig. 8; Fig. 10). The majority of species had producer and user's accuracy distributions that were significantly different from the single date classifications (Figs. S11–S14). For seasonal libraries, approximately 58% of species' accuracies were negatively impacted compared to single date libraries with producer and user accuracies dropping by 3.8 and 4% on average. Yearly libraries had a similar response with 59% of species having lower accuracies, with user accuracy dropping by 4.1% and producer accuracy by 4% on average. Use of the All-Dates spectral library for classification increased the number of species negatively impacted to 67%. User accuracies dropped on average by 7.4% and producer accuracies by 7.7% compared to single date classifications. While a majority of species across dates were negatively impacted with the inclusion of additional spectra, others experienced an increase in classification accuracy using multiple-date libraries or were not significantly different. Approximately 25% of the species for seasonal and yearly libraries and 19% of the species for All-Dates library did not have significantly different accuracies compared to the single date spectral library. Fig. 10 shows an example of the variation described above for three species in two image dates. We did not find a single species across dates or an image date across species that consistently performed better or worse using multiple date spectral libraries.

3.3. LOO spectral libraries

To test the transferability of spectral libraries, we developed leave-one-out (LOO) cross-validation spectral libraries to classify image dates (Table 6). Classification accuracies of images using these libraries were significantly lower than the single date or multiple date spectral libraries. An image was not classified well unless spectra from that image were contained in the spectral library. The best performing LOO spectral library was the 2015 Summer imagery with a mean kappa of 0.73, but this was still significantly lower than the single date or multiple date spectral libraries' classification accuracies (mean kappa range from 0.78 to 0.86). The lowest performing was the 2014 Summer imagery with a mean kappa of 0.31, demonstrating that spectra from this image date were the least similar to other dates. This date also corresponds to the peak of the California drought.

In general, the loss of classification accuracy was also true for individual plant species' user and producer accuracies (Fig. 8; Fig. 10; Figs. S11–S14). Compared to the single date spectral libraries, approximately 73% of species across dates had lower classification accuracies using LOO spectral libraries. We found that the Spring 2013 and Summer 2014 image classification suffered the most when using LOO spectral libraries. Spring 2015 imagery was the least impacted using LOO libraries but was only marginally better than other image dates. While most species generally performed worse using LOO spectral libraries, the magnitude of loss depended on the image date and species. For example, for ARCA-SALE, a top performing species for other libraries, the mean classification accuracy dropped by 40% from Spring 2013 to Fall 2013 imagery using the LOO spectral libraries

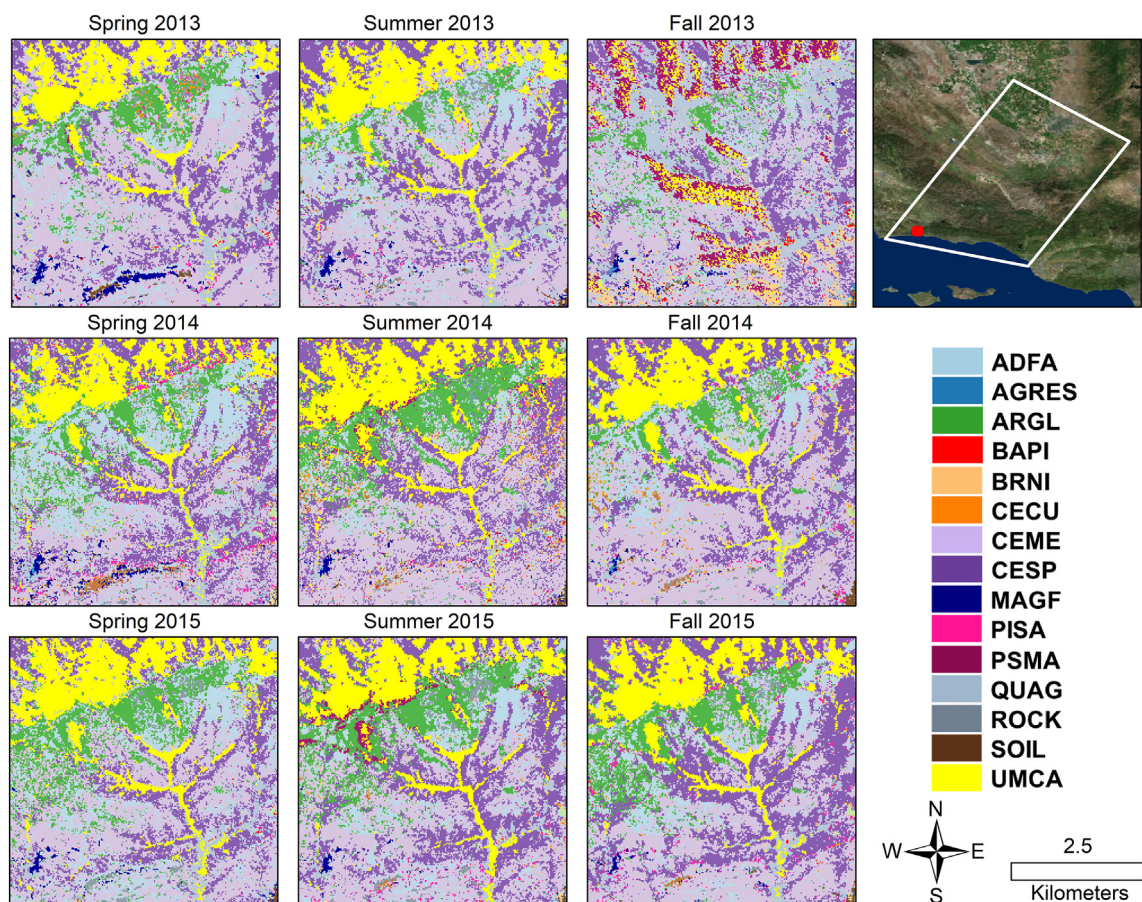


Fig. 6. Plant species classifications zoomed in on a portion of the Santa Ynez Mountain foothills. Only species and classes present in this subset are included in the legend.

(Fig. 10). However, for Summer 2015 and Fall 2015 imagery, the classification accuracies only differed by 5%.

4. Discussion

4.1. Classifying plant species

To establish baseline classification capabilities, we classified plant species using spectra from a single image date. We found that plant species can be classified across this diverse landscape with a mean kappa accuracy ranging from 0.78 to 0.84 over the nine image dates. These results demonstrate that California plant species, often found in remote and rugged terrain, can be classified accurately using hyperspectral remote sensing. Additionally, this study was able to classify species with user and producer's accuracies > 75%, even though most represent less than ideal characteristics for remotely classifying. The species analyzed in this study were predominantly chaparral shrubs or conifers, for which many individuals are required to fill a single 18 m pixel. Many of these species grow in heterogeneous patches with individuals from other species influencing the spectrum. Some species in this study are dispersed on the landscape or do not form dense canopies, which introduces substrate influence into the spectrum. In contrast, other classification studies focusing on broadleaf tree species often have a single individual that can fill an entire pixel, resulting in a spectrum composed of solely that individual. For example, *Juniper californica* (JUCA), a shrub with open canopies that do not fill an entire 18 m pixel, had a mean producer and user accuracy of 79.4 and 63.9% for Spring 2013 imagery. Meanwhile, *Quercus douglasii* (QUDO) had a mean producer and user accuracy of 94.7 and 92.1% for Spring 2013 imagery because it is a broadleaf large canopy tree and filled the entire

pixel.

Other studies have also had success mapping plant species using a single date spectral library. In a subset of our study area, Roth et al., 2015b, 2015a classified 23 dominant chaparral plant species with a 0.84 mean kappa accuracy, also using CDA-LDA as a classifier. Roberts et al. (2015) also classified 22 of the same classes as reported in this study with a kappa accuracy of 0.73 using Multiple Endmember Spectral Mixture Analysis (MESMA). In other ecosystems, a single date spectral library has been used to classify plant species with a range of success using different methodologies. For example, three southern pine species in North America were mapped with 83% accuracy (van Aardt and Wynne, 2007), eleven eastern broadleaf tree species in North America were classified with 75% accuracy (Martin et al., 1998), and seven tropical rainforest species were classified with 92% accuracy (Clark et al., 2005). The results of this study complement the studies mentioned above and establish our capabilities for classifying plant species using airborne datasets. The next step in determining the possibility of classifying species with future hyperspectral satellites is evaluating our classification capabilities across time.

4.2. Annual and seasonal classification of plant species

We explored the potential for using a multi-temporal spectral library for classification that would be better suited for capturing the variability anticipated by the HyspIRI sensor. The seasonal and annual spectral libraries performed similarly to single-date spectral library classifications with a slight decrease in accuracy. In general, seasonal libraries performed better than yearly libraries, demonstrating that matching phenology plays a dominant role in species classification. Including spectra from all nine image dates further decreased kappa

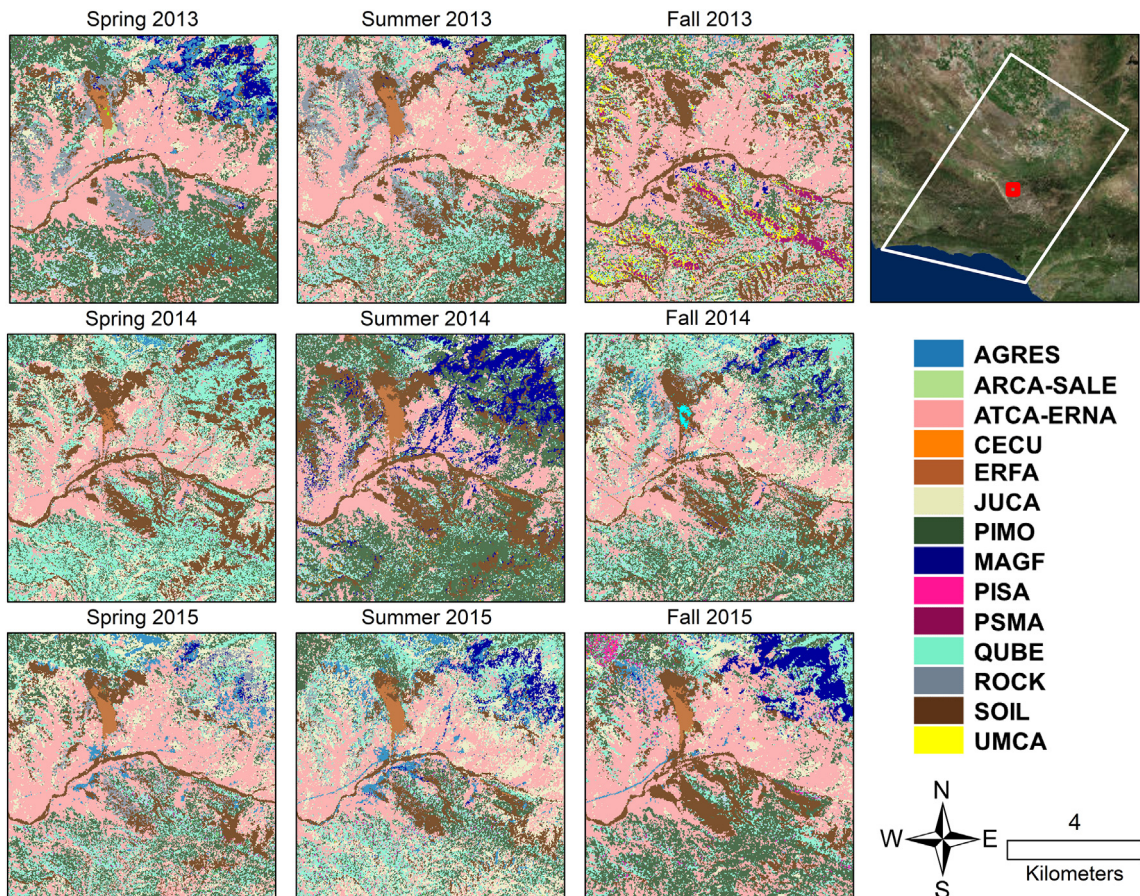


Fig. 7. Plant species classifications zoomed in on a portion of the Los Padres National Forest. Only species and classes present in this subset are included in the legend.

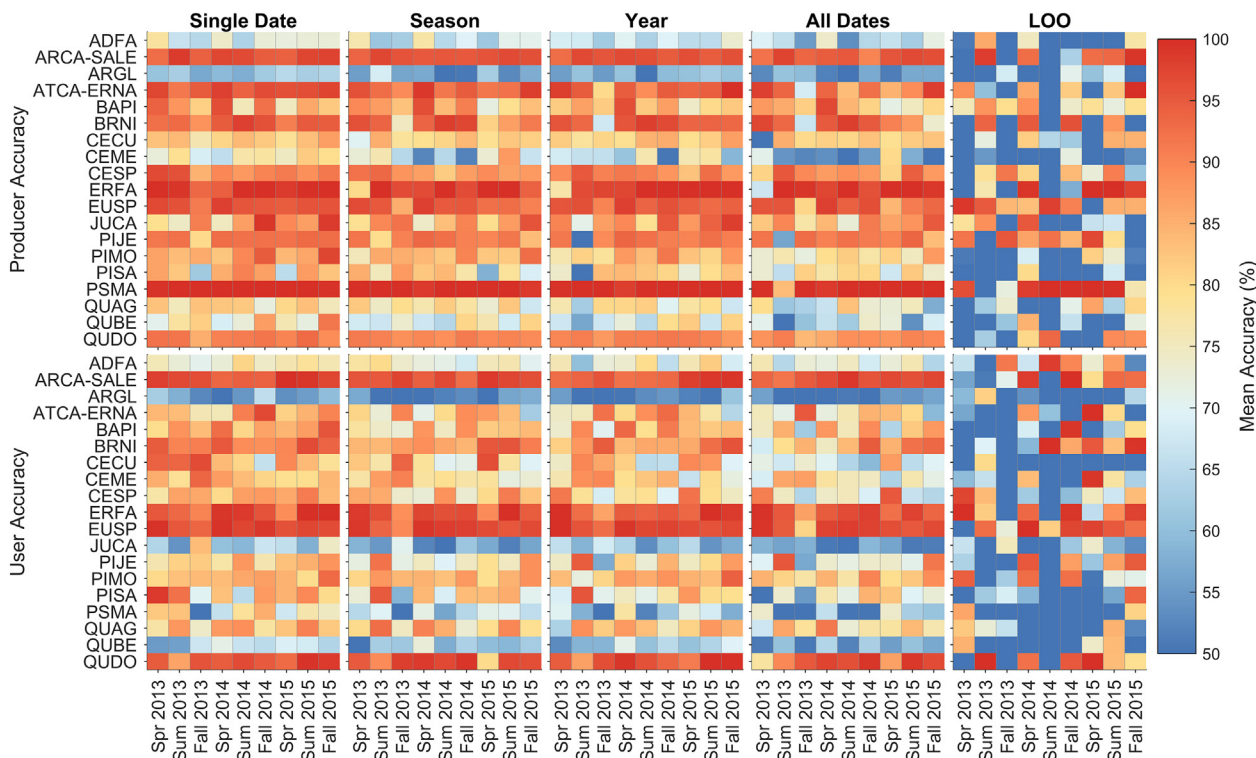


Fig. 8. Mean producer and user's accuracies using different spectral libraries on the nine image dates. Classes missing from the figure are AGRES, CISP, IRGR, MAGF, PEAM, ROCK, SOIL, and UMCA. All classes' accuracies found in Figs. S11–S14.

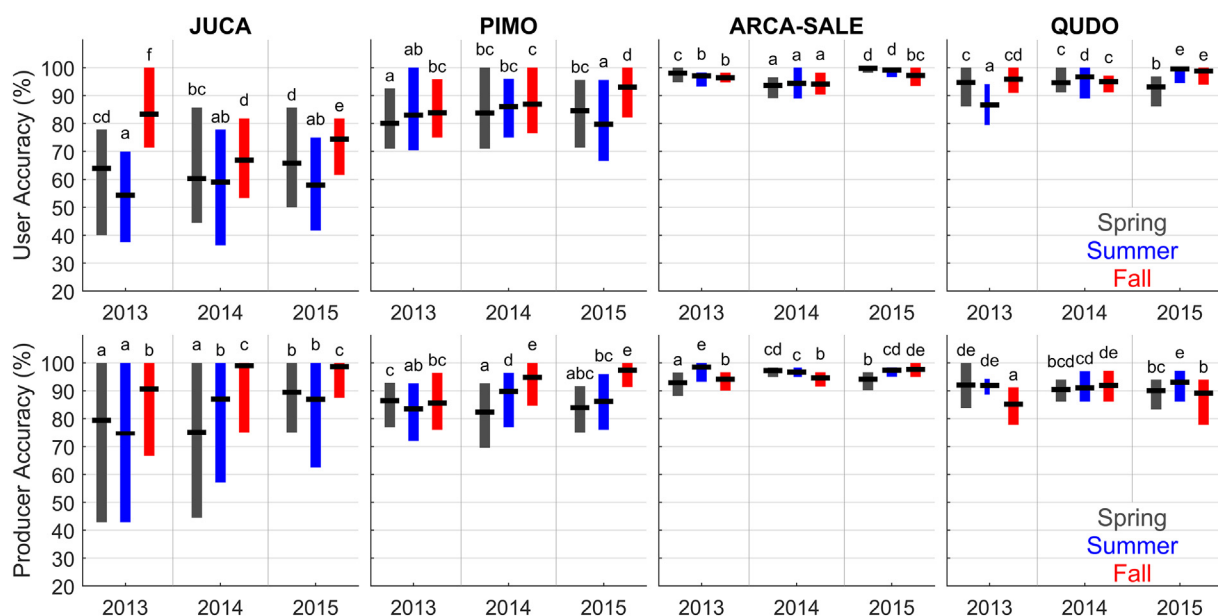


Fig. 9. Comparison of four classes' user and producer accuracies across image dates using single date spectral libraries. JUCA and PIMO were the lowest performing, and ARCA-SALE and QUDO were the highest performing classes. Dots are mean accuracy with the top and bottom of bars marking the maximum and minimum accuracies across 50 iterations. Letters designate which of the nine dates are significantly different for a single species ($p < 0.05$).

classification by adding too much seasonal and annual spectral variability. In other disciplines, an increased amount of data results in more accurate or representative models, whereas in vegetation remote sensing it does not. While species do exhibit unique spectral characteristics due to biochemical and structural composition, individuals can deviate from the normal, creating a distribution of potential spectra for a species (Asner and Martin, 2009). These distributions can overlap other species' spectral distributions, particularly as the variability of seasonal and year-to-year changes in a species' spectral response are added. In our study, that added variability ultimately reduced spectral separability between classes and confused the classifier.

From 2012 to 2015, California experienced conditions that resulted in the most severe drought over the past 1200 years of tree ring data (Griffin and Anchukaitis, 2014). During this time, the state's 12-month accumulated precipitation was $< 34\%$ of average, resulting in the hottest and driest year in the full instrumental record which started 1895 (Mann and Gleick, 2015; Swain et al., 2014). Our imagery was collected during this drought and captured plants adversely affected by drought. Drought changes a plant species' spectral response as canopy water content decreases (Asner et al., 2004; Martin et al., 2018; Ustin et al., 1998). In this study, the variability in a plant's spectra was not only impacted by phenology, but also by drought. Results of the annual and seasonal library classifications may have had lower accuracies due to the introduced variability of the drought, which compounds variability observed between species due to altered phenology compared to

previous years. In addition, the libraries might have resulted in lower accuracies because they were not representative of the phenology on the ground. Fig. 2 shows how the timing of phenological events varied from year to year, which means imagery did not capture the same phenology stage between collection dates. For example, plants in 2014 experienced different phenological patterns than in 2013 and 2015. Our seasonal and annual classifications were trained using all three years, which might have added variability that ultimately confused the classifier and decreased accuracy. We chose to divide our spectral libraries by calendar years, but future work should develop a methodology to select spectral libraries for classification that are based on plant phenology.

Very few studies have explored plant species classification through seasons or years at the canopy scale. However, phenological patterns have been found to be important factors at the leaf level with hyperspectral measurements. In tropical forests, Hesketh and Sánchez-Azofeifa (2012) found that the classification of trees and lianas at the leaf level dropped from approximately 80% accuracy for a single season to 20% across seasons. Burkholder et al. (2011) found that the ability to separate invasive and native species at the leaf level peaked in July and August, when optimum band selection shifted between each sampling period. When discriminating reed species, Fernandes et al. (2013) found that species are only spectrally distinct during the senescent period. These studies emphasize the importance of capturing species distributions as they change across seasons and years, not only in a

Table 5

Average classification kappa accuracy for each image date using multi-date spectral libraries. Averaged kappa accuracy is calculated from 50 iterations. Bold designates spectral libraries that contain image date spectra. Rows report the spectral library, while columns report image dates.

	Image date								
	Spr 2013	Sum 2013	Fall 2013	Spr 2014	Sum 2014	Fall 2014	Spr 2015	Sum 2015	Fall 2015
Spr-All	0.83	0.62	0.36	0.82	0.27	0.38	0.79	0.55	0.42
Sum-All	0.38	0.82	0.34	0.57	0.81	0.65	0.47	0.83	0.58
Fall-All	0.20	0.51	0.79	0.37	0.16	0.80	0.41	0.52	0.79
2013-All	0.80	0.79	0.78	0.30	0.14	0.36	0.42	0.30	0.35
2014-All	0.28	0.42	0.31	0.83	0.81	0.80	0.58	0.64	0.66
2015-All	0.09	0.10	0.17	0.59	0.20	0.52	0.82	0.83	0.81
All-Dates	0.76	0.78	0.72	0.80	0.77	0.79	0.78	0.79	0.77

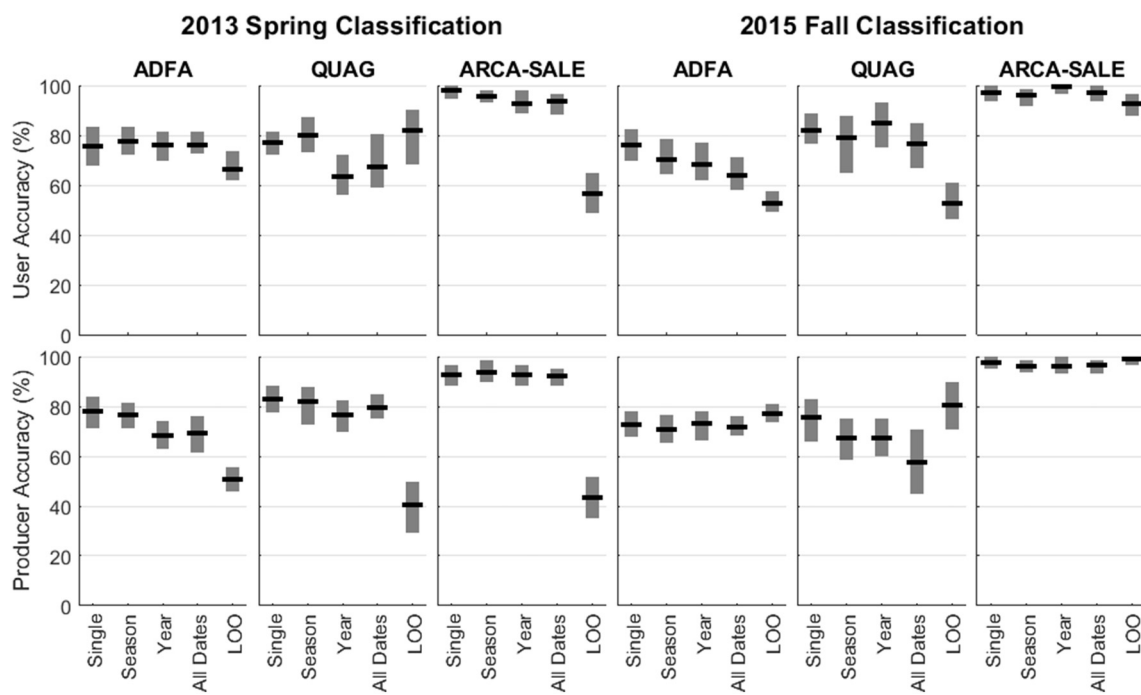


Fig. 10. Comparison of three species' producer and user accuracies for two image dates using five different spectral libraries. Horizontal black lines mark mean accuracy with the top and bottom of bars marking the maximum and minimum accuracies across 50 iterations.

single observation.

Only five published studies have classified plant species across multiple dates. Using five water deficit image dates, [Dennison and Roberts \(2003\)](#) found that the amount of variation in non-photosynthetic materials increased confusion between species and ultimately decreased accuracy by 8–16%. Conversely, additional research found that the inclusion of monthly spectra increased detection by 0.11–0.29 kappa for invasive tree species in Hawaii using Earth Observing-1 Hyperion data ([Somers and Asner, 2013, 2012](#)). Classifying tree species in French Guiana, [Laybros et al. \(2019\)](#) reported that accuracy dropped from 75.9 kappa with single date classification to 65.6 kappa with classification trained on one date and applied to another. [Dudley et al. \(2015\)](#), using five image dates from a single year, found that seasonally-mixed spectral libraries achieved similar overall classification accuracies compared to single-date libraries, and in some cases, resulted in improved classification accuracies. While similar to our study, the study by [Dudley et al. \(2015\)](#) had critical differences including a smaller study area, finer spatial resolution (10.9–16.7 m), and imagery only from a single year, compared to our study which includes a 12,980 km² area, 18 m spatial resolution, and three years of imagery.

4.3. Transferability of plant species classification

The collection and processing of reference spectra are time-consuming and expensive steps. Ideally, reference spectra that can be shared across geographies and dates would vastly improve the efficiency of remote sensing applications. Our analysis used LOO spectral libraries to test the transferability of spectral libraries. We found that classification accuracy dropped severely if spectra from the image date were not included in the spectral library. The LOO spectral libraries decreased mean kappa accuracy to 0.31–0.73 compared to the single date spectral library with a mean kappa of 0.80–0.86. The variability in classification accuracy across the 50 iterations also increased significantly compared to other libraries. For this study area and dates observed, we found that spectral libraries were not transferrable across dates. We hypothesize this is due to changing phenology and environmental conditions captured during collection. The airborne dataset was acquired over 4–6 h with variable sun-sensor geometry and captured during increasing drought conditions. Perhaps under similar conditions of soil moisture and lighting, spectral libraries would be transferrable across dates. The limited ability to transfer spectral libraries across dates is restricted to biotic materials. Abiotic materials, e.g., rocks, minerals, and urban materials, are portable across time because they

Table 6

Mean classification kappa accuracy for each image date using leave-one-out (LOO) spectral libraries. Mean kappa accuracy is calculated from 50 iterations. Bold designates spectral library that does not contain image date spectra. Rows report the spectral library, while columns report image dates.

	Image date								
	Spr 2013	Sum 2013	Fall 2013	Spr 2014	Sum 2014	Fall 2014	Spr 2015	Sum 2015	Fall 2015
LOO-Spr13	0.47	0.78	0.74	0.79	0.77	0.79	0.78	0.79	0.77
LOO-Sum13	0.78	0.61	0.73	0.79	0.78	0.78	0.78	0.79	0.77
LOO-Fall13	0.78	0.79	0.44	0.80	0.79	0.79	0.79	0.81	0.78
LOO-Spr14	0.77	0.78	0.73	0.67	0.77	0.80	0.79	0.79	0.77
LOO-Sum14	0.77	0.78	0.73	0.80	0.31	0.79	0.78	0.79	0.77
LOO-Fall14	0.77	0.78	0.73	0.79	0.77	0.59	0.78	0.79	0.76
LOO-Spr15	0.77	0.78	0.74	0.80	0.78	0.79	0.61	0.79	0.77
LOO-Sum15	0.76	0.78	0.73	0.80	0.78	0.79	0.78	0.73	0.76
LOO-Fall15	0.77	0.78	0.74	0.80	0.78	0.79	0.78	0.79	0.64

are generally invariant (Herold et al., 2004; Herold and Roberts, 2005).

The scientific community has been developing databases of spectra to assist remote sensing applications for many decades. Most spectral libraries with plant species focus on leaf or canopy spectra collected with a handheld spectrometer, but a couple of libraries contain image-derived spectra. One of the most recently developed spectral libraries is the NASA-funded Ecosystem Spectral Information System (EcoSIS) spectral library that hosts spectra which are uploaded by researchers and are publicly available for download (<https://ecosis.org/>). The scientific community has long recognized the usefulness of spectral libraries for reducing analysis and processing time (e.g., Baldridge et al., 2009; Herold et al., 2004; Hueni et al., 2009; Zomer et al., 2009).

However, databases of spectra can prove challenging to transfer to a new study area, time frame, or image source (Herold et al., 2004; Wetherley et al., 2017). It can also be difficult to find existing spectral libraries that capture a similar climatic or temporal period for a new research area (Das et al., 2015; Herold and Roberts, 2005). From our research, it is apparent that image derived spectra will likely not be transferrable to a new image date, meaning that existing spectral libraries will likely not yield accurate classifications. Instead, we believe there is a need for starting a public geodatabase of reference polygons and locations of species and classes that can be used for any research application, sensor, or time period. The development of such a database would provide a validation and training dataset that can be used across all remote sensing platforms for any application. This database, in addition to databases of spectra, would provide researchers full flexibility for future projects across sensors and time periods. However, this dataset would need to be periodically validated to confirm polygons still represent the classes for which they are intended. This is especially true as species' distributions may shift due to climate change, extreme events, or natural succession.

4.4. Challenges and opportunities when using airborne hyperspectral imagery

While this study is a reasonable representation of the data that will be available with HyspIRI, there are some additional considerations to take into account, specifically including spatial resolution, georeferencing, and atmospheric correction. Currently, the proposed spatial resolution of HyspIRI is 30 m pixels, while this study used 18 m pixels. Spatial resolution has been found to affect classification accuracy and would need to be further investigated (Roth et al., 2015a; Schaaf et al., 2011). Furthermore, at the HyspIRI scale, spaceborne missions tend to deliver stable image geolocation at a subpixel level, which is not available with airborne passive remote sensing. To mitigate these differences, we made extensive efforts to reference AVIRIS images to known ground locations and also aligned the images between dates. However, geolocation errors are still present in the dataset due to residual misalignment. Finally, the reflectance retrieval algorithm was evolving as the campaign progressed, which influenced the stability in reflectance between images. We attempted to correct for spectral differences between dates and flight lines by using an invariant reflectance target, but some spectral differences that are caused by the reflectance retrieval, and not species phenology, may still exist. BRDF effects on imagery are a common issue with airborne platforms and were shown to impact this dataset study and other studies using this dataset (Tane et al., 2018a; Wetherley et al., 2017). Also, BRDF effects on this dataset are further exacerbated by multi-hour imaging campaigns required to cover each flight box. In HyspIRI images spaced by 19 days, the fixed viewing geometry and rapid image acquisition will reduce BRDF differences within a scene and across dates, thus potentially improving classification accuracy compared to the HyspIRI-like airborne imagery.

Identifying capabilities of mapping plant species presents opportunities for sensors currently or soon-to-be deployed in addition to HyspIRI. For example, scheduled to launch in 2019, the Environmental Mapping and Analysis Program (EnMAP) mission sponsored by

Germany is an imaging spectrometer that will provide measurements at 420–1000 nm and 900–2450 nm (Stuffler et al., 2007). This mission would provide global coverage with a revisit time of 27 days, and would significantly increase hyperspectral data volume for temporal classification of species. In addition, the National Ecological Observatory Network (NEON) airborne mission flies an imaging spectrometer once a year over 47 terrestrial field sites (Kampe et al., 2010). Sponsored by the National Science Foundation, this program is expected to continue for 30 years, which will yield the largest imaging spectroscopy dataset with continuous measurements for individual locations. The results of this study provide a link between existing research and future possibilities for classifying plant species across seasons over the years using datasets such as HyspIRI, EnMAP, and NEON.

5. Conclusion

Our study quantifies the potential for classifying seasonal and yearly distributions of plant species, specifically for the HyspIRI sensor. We set out to answer three questions. First, we asked how accurately can plant species be classified across spring, summer, and fall in 2013–2015 using single date spectral libraries. We found that the 27 species and land cover types in this study were classified with high accuracies across the nine dates (mean kappa 0.80–0.86). Species with open canopies had the lowest user and producer accuracies because of the influence of the substrate on spectra. Second, we explored the use of multiple date spectral libraries for classification to capture a broader range of phenological conditions that would be present in the repeat acquisitions of the HyspIRI mission. We found that the increased spectral variability due to changes in plant phenology and drought conditions, and perhaps the combined errors of various preprocessing steps that are unique to the airborne image data used, resulted in a loss of classification accuracy. However, accuracies were still comparable to single date libraries with seasonal libraries having a mean kappa 0.79–0.83 and annual libraries having a mean kappa 0.78–0.83. Finally, we asked how transferrable vegetation spectral libraries are across dates using LOO spectral libraries. We found that LOO libraries resulted in a significant decrease in classification accuracy (mean kappa 0.31–0.73) and did not yield species maps that would be accurate enough for future research. However, this might not be true for satellite-based measurements, which will have a smaller range of sun-sensor geometries compared to the airborne dataset.

Instead of developing image-based vegetation spectral libraries, we recommend that the science community develop a geodatabase containing reference locations of species that can then be applied to any image or sensor. Such a database would allow researchers flexibility in addressing science questions. This flexibility is crucial as temporal hyperspectral datasets grow exponentially with ongoing airborne campaigns and proposed spaceborne missions. The proposed HyspIRI mission would be uniquely poised to capture plant species distributions with a 19-day revisit time globally. Thus, it is essential to expedite the development of robust multi-temporal species classification techniques capable of extracting new information from the temporal dimension of hyperspectral data.

Acknowledgments

We want to acknowledge S. Lucille Blakeley, Alexander Preston, Rafael Ramos, and Kelly Caylor for their comments throughout the development of this manuscript. This project was supported by a NASA Grant NNX12AP08G, *HyspIRI discrimination of plant species and functional types along a strong environmental-temperature gradient* and a NASA Earth and Space Science Fellowship (NESSF). The project was also partially supported by the Harris Corporation. We also thank two anonymous reviewers and Editor Dr. Chuvieco for helpful comments that improved the manuscript.

Appendix A. Supplementary data

Supplementary data to this article can be found online at <https://doi.org/10.1016/j.rse.2019.111308>.

References

- van Aardt, J., Wynne, R.H., 2007. Examining pine spectral separability using hyperspectral data from an airborne sensor: an extension of field based results. *Int. J. Remote Sens.* 28, 431–436. <https://doi.org/10.1080/01431160500444772>.
- Alonzo, M., Roth, K.L., Roberts, D.A., 2013. Identifying Santa Barbara's urban tree species from AVIRIS imagery using canonical discriminant analysis. *Remote Sens. Lett.* 4, 513–521. <https://doi.org/10.1080/2150704X.2013.764027>.
- Asner, G.P., Martin, R.E., 2008. Spectral and chemical analysis of tropical forests: scaling from leaf to canopy levels. *Remote Sens. Environ.* 112, 3958–3970. <https://doi.org/10.1016/j.rse.2008.07.003>.
- Asner, G.P., Martin, R.E., 2009. Airborne spectronomics: mapping canopy chemical and taxonomic diversity in tropical forests. *Front. Ecol. Environ.* 7, 269–276. <https://doi.org/10.1890/070152>.
- Asner, G.P., Nepstad, D., Cardinot, G., Ray, D., 2004. Drought stress and carbon uptake in an Amazon forest measured with spaceborne imaging spectroscopy. *Proc. Natl. Acad. Sci.* 101, 6039–6044. <https://doi.org/10.1073/pnas.0400168101>.
- Baldridge, A.M., Hook, S.J., Grove, C.I., Rivera, G., 2009. The ASTER spectral library version 2.0. *Remote Sens. Environ.* 113, 711–715. <https://doi.org/10.1016/j.rse.2008.11.007>.
- Bell, T.W., Cavanaugh, K.C., Siegel, D.A., 2015. Remote monitoring of giant kelp biomass and physiological condition: an evaluation of the potential for the Hyperspectral Infrared Imager (HypIRI) mission. *Remote Sens. Environ.* 167, 218–228. <https://doi.org/10.1016/j.rse.2015.05.003>.
- Burkholder, A., Warner, T.A., Culp, M., Landenburg, R., 2011. Seasonal trends in separability of leaf reflectance spectra for *Ailanthus altissima* and four other tree species. *Photogramm. Eng. Remote Sensing* 77, 793–804. <https://doi.org/10.14358/PERS.77.8.793>.
- Clark, R.N., Swazy, G.A., Livo, K.E., Kokaly, R.F., King, T.V.V., Dalton, J.B., Vance, J.S., Rockwell, B.W., Hoefen, T., McDougal, R.R., 2002. Surface reflectance calibration of terrestrial imaging spectroscopy data: a tutorial using AVIRIS. In: *Proc. 10th Airborne Earth Sci. Work*, pp. 1–21.
- Clark, M.L., Roberts, D.A., Clark, D.B., 2005. Hyperspectral discrimination of tropical rain forest tree species at leaf to crown scales. *Remote Sens. Environ.* 96, 375–398. <https://doi.org/10.1016/j.rse.2005.03.009>.
- Cleland, E.E., Chuine, I., Menzel, A., Mooney, H.A., Schwartz, M.D., 2007. Shifting plant phenology in response to global change. *Trends Ecol. Evol.* 22, 357–365. <https://doi.org/10.1016/j.tree.2007.04.003>.
- Coates, A., Dennison, P., Roberts, D., Roth, K., 2015. Monitoring the impacts of severe drought on southern California chaparral species using hyperspectral and thermal infrared imagery. *Remote Sens.* 7, 14276–14291. <https://doi.org/10.3390/rs71114276>.
- Cohen, W.B., Goward, S.N., 2004. Landsat's Role in Ecological Applications of Remote Sensing. *BioScience* 54 (6), 535. [https://doi.org/10.1641/0006-3568\(2004\)054\[0535:LRIEAO\]2.0.CO;2](https://doi.org/10.1641/0006-3568(2004)054[0535:LRIEAO]2.0.CO;2).
- Congalton, R.G., 1991. A review of assessing the accuracy of classifications of remotely sensed data. *Remote Sens. Environ.* 37, 35–46. [https://doi.org/10.1016/0034-4257\(91\)90048-B](https://doi.org/10.1016/0034-4257(91)90048-B).
- Cruz-Castillo, J.G., Ganeshanandam, S., Mackay, B.R., Lawes, G.S., Lawoko, C.R.O., Woolley, D.J., 1994. Applications of canonical discriminant analysis in horticultural research. *Hortic. Sci.* 29, 1115–1119.
- Das, B.S., Ray, S.S., Sarathjith, M.C., Santra, P., Sahoo, R.N., Srivastava, R., 2015. Hyperspectral remote sensing: opportunities, status and challenges for rapid soil assessment in India. *Curr. Sci.* 108, 860–868.
- Davis, F.W., Michaelsen, J., 1995. Sensitivity of fire regime in chaparral ecosystems to climate change. In: J.M., M., W.C., O. (Eds.), *Global Change and Mediterranean-type Ecosystems*. volume 117. Springer, New York, NY, pp. 435–456. https://doi.org/10.1007/978-1-4612-4186-7_21.
- Dennison, P.E., Roberts, D.A., 2003. The effects of vegetation phenology on endmember selection and species mapping in southern California chaparral. *Remote Sens. Environ.* 87, 295–309. <https://doi.org/10.1016/j.rse.2003.07.001>.
- Dennison, P.E., Roberts, D.A., Thorgersen, S.R., Regelbrugge, J.C., Weise, D., Lee, C., 2003. Modeling seasonal changes in live fuel moisture and equivalent water thickness using a cumulative water balance index. *Remote Sens. Environ.* 88, 442–452. <https://doi.org/10.1016/j.rse.2003.08.015>.
- Diamond, H.J., Karl, T.R., Palecki, M.A., Baker, C.B., Bell, J.E., Leeper, R.D., Easterling, D.R., Lawrimore, J.H., Meyers, T.P., Helfert, M.R., Goodge, G., Throne, P.W., 2013. U.S. climate reference network after one decade of operations: status and assessment. *Am. Meteorol. Soc.* 485–498. <https://doi.org/10.1175/BAMS-D-12-00170.1>.
- Dudley, K.L., Dennison, P.E., Roth, K.L., Roberts, D.A., Coates, A.R., 2015. A multi-temporal spectral library approach for mapping vegetation species across spatial and temporal phenological gradients. *Remote Sens. Environ.* 167, 121–134. <https://doi.org/10.1016/j.rse.2015.05.004>.
- Fernandes, M.R., Aguiar, F.C., Silva, J.M.N., Ferreira, M.T., Pereira, J.M.C., 2013. Spectral discrimination of giant reed (*Arundo donax* L.): a seasonal study in riparian areas. *ISPRS J. Photogramm. Remote Sens.* 80, 80–90. <https://doi.org/10.1016/j.isprsjprs.2013.03.007>.
- Fisher, R., 1936. The use of multiple measurements in taxonomic problems. *Ann. Eugenics* 7, 179–188. <https://doi.org/10.1111/j.1469-1809.1936.tb02137.x>.
- George, R., Padalia, H., Kushwaha, S.P.S., 2014. Forest tree species discrimination in western Himalaya using EO-1 Hyperion. *Int. J. Appl. Earth Obs. Geoinf.* 28, 140–149. <https://doi.org/10.1016/j.jag.2013.11.011>.
- Gill, D.S., Mahall, B.E., 1986. Quantitative phenology and water relations of an evergreen and a deciduous chaparral shrub. *Ecol. Monogr.* 56, 127–143.
- Green, R.O., Pavri, B., Faust, J., Williams, O., 1998. AVIRIS Radiometric Laboratory Calibration, Inflight Validation and a Focused Sensitivity Analysis in 1998. *JPL Publication*.
- Griffin, D., Anchukaitis, K.J., 2014. How unusual is the 2012–2014 California drought? *Geophys. Res. Lett.* 41, 9017–9023. <https://doi.org/10.1002/2014GL062433.1>.
- He, T., Liang, S., Wang, D., Shi, Q., Goulden, M.L., 2015. Estimation of high-resolution land surface net shortwave radiation from AVIRIS data: algorithm development and preliminary results. *Remote Sens. Environ.* 167, 20–30. <https://doi.org/10.1016/j.rse.2015.03.021>.
- Herold, M., Roberts, D., 2005. Spectral characteristics of asphalt road aging and deterioration: implications for remote-sensing applications. *Appl. Opt.* 44, 4327–4334. <https://doi.org/10.1364/AO.44.004327>.
- Herold, M., Roberts, D.A., Gardner, M.E., Dennison, P.E., 2004. Spectrometry for urban area remote sensing – development and analysis of a spectral library from 350 to 2400 nm. *Remote Sens. Environ.* 91, 304–319. <https://doi.org/10.1016/j.rse.2004.02.013>.
- Hesketh, M., Sánchez-Azofeifa, G.A., 2012. The effect of seasonal spectral variation on species classification in the Panamanian tropical forest. *Remote Sens. Environ.* 118, 73–82. <https://doi.org/10.1016/j.rse.2011.11.005>.
- Hueni, A., Nieke, J., Schopfer, J., Kneubühler, M., Itten, K.I., 2009. The spectral database SPECCHIO for improved long-term usability and data sharing. *Comput. Geosci.* 35, 557–565. <https://doi.org/10.1016/j.cageo.2008.03.015>.
- Hufstader, R.W., 1978. Growth rates and phenology of some southern California grassland species. *J. Range Manag.* 31, 465. <https://doi.org/10.2307/3897208>.
- Irani, M., 2002. Multi-frame correspondence estimation using subspace constraints. *Int. J. Comput. Vis.* 48, 173–194.
- Kampe, T.U., Johnson, B.R., Kuester, M., Keller, M., 2010. NEON: the first continental-scale ecological observatory with airborne remote sensing of vegetation canopy biochemistry and structure. *J. Appl. Remote. Sens.* 4. <https://doi.org/10.1117/1.3361375>.
- Kelly, A.E., Goulden, M.L., 2008. Rapid shifts in plant distribution with recent climate change. *Proc. Natl. Acad. Sci. U. S. A.* 105, 11823–11826. <https://doi.org/10.1073/pnas.0802891105>.
- Khanna, S., Santos, M.J., Ustin, S.L., Koltunov, A., Kokaly, R.F., Roberts, D.A., 2013. Detection of salt marsh vegetation stress and recovery after the Deepwater Horizon Oil Spill in Barataria Bay, Gulf of Mexico using AVIRIS data. *PLoS One* 8, e78989. <https://doi.org/10.1371/journal.pone.0078989>.
- Khanna, S., Santos, M.J., Koltunov, A., Shapiro, K.D., Lay, M., Ustin, S.L., 2017. Marsh loss due to cumulative impacts of hurricane isaac and the DeepWater Horizon oil spill in Louisiana. *Remote Sens.* 9, 1–18. <https://doi.org/10.3390/rs9020169>.
- Klecka, W., 1980. *Discriminant Analysis*. Sage Publications.
- Koedsin, W., Vaiphana, C., 2013. Discrimination of tropical mangroves at the species level with EO-1 hyperion data. *Remote Sens.* 5, 3562–3582. <https://doi.org/10.3390/rs5073562>.
- Koltunov, A., Ben-Dor, E., Ustin, S.L., 2009. Image construction using multitemporal observations and dynamic detection models. *Int. J. Remote Sens.* 30, 57–83. <https://doi.org/10.1080/01431160802220193>.
- Koltunov, A., Ustin, S.L., Quayle, B., Schwind, B., 2012. GOES early fire detection (GOES-EFD) system prototype. In: *ASPRS 2012 Annual Conference*, pp. 1–10 Sacramento, CA.
- Koltunov, A., Ustin, S.L., Quayle, B., Schwind, B., Ambrosia, V.G., Li, W., 2016. The development and first validation of the GOES Early Fire Detection (GOES-EFD) algorithm. *Remote Sens. Environ.* 184, 436–453. <https://doi.org/10.1016/j.rse.2016.07.021>.
- Lawrence, R., Labus, M., 2003. Early detection of Douglas-fir beetle infestation with subcanopy resolution hyperspectral imagery. *J. Appl. For.* 18, 1–5.
- Laybros, A., Schläpfer, D., Féret, J., Descroix, L., Bedreau, C., Lefèvre, M., Vincent, G., 2019. Across date species detection using airborne imaging spectroscopy. *Remote Sens.* 11, 1–24. <https://doi.org/10.3390/rs11070789>.
- Lee, C.M., Cable, M.L., Hook, S.J., Green, R.O., Ustin, S.L., Mandl, D.J., Middleton, E.M., 2015. An introduction to the NASA Hyperspectral InfraRed Imager (HypIRI) mission and preparatory activities. *Remote Sens. Environ.* 167, 6–19. <https://doi.org/10.1016/j.rse.2015.06.012>.
- Mann, M.E., Gleick, P.H., 2015. Climate change and California drought in the 21st century. *Proc. Natl. Acad. Sci.* 112, 3858–3859. <https://doi.org/10.1073/pnas.1503667112>.
- Martin, M.E., Newman, S., Aber, J.D., Congalton, R., 1998. Determining forest species composition using high spectral resolution remote sensing data. *Remote Sens. Environ.* 65, 249–254. [https://doi.org/10.1016/S0034-4257\(98\)00035-2](https://doi.org/10.1016/S0034-4257(98)00035-2).
- Martin, R.E., Asner, G.P., Francis, E., Ambrose, A., Baxter, W., Das, A.J., Vaughn, N.R., Paz-Kagan, T., Dawson, T., Nydick, K., Stephenson, N.L., 2018. Remote measurement of canopy water content in giant sequoias (*Sequoiadendron giganteum*) during drought. *For. Ecol. Manag.* 419–420, 279–290. <https://doi.org/10.1016/j.foreco.2017.12.002>.
- Meentemeyer, R.K., Moody, A., Franklin, J., 2001. Landscape-scale patterns of shrub-subspecies abundance in California chaparral. *Plant Ecol.* 156, 19–41. <https://doi.org/10.1023/A:1011944805738>.
- National Academies of Sciences and Medicine, E., 2018. *Thriving on Our Changing Planet: A Decadal Strategy for Earth Observation From Space*. The National Academies Press, Washington, DC. <https://doi.org/10.17226/24938>.
- Palacios, S.L., Kudela, R.M., Guild, L.S., Negrey, K.H., Torres-Perez, J., Broughton, J., 2015. Remote sensing of phytoplankton functional types in the coastal ocean from

- the HypPIRI Preparatory Flight Campaign. *Remote Sens. Environ.* 167, 269–280. <https://doi.org/10.1016/j.rse.2015.05.014>.
- Peñuelas, J., Filella, I., 1998. Visible and near-infrared reflectance techniques for diagnosing plant physiological status. *Trends Plant Sci.* 3, 151–156. [https://doi.org/10.1016/S1360-1385\(98\)01213-8](https://doi.org/10.1016/S1360-1385(98)01213-8).
- Riaño, D., Chuvieco, E., Ustin, S.L., Zomer, R., Dennison, P.E., Roberts, D.A., Salas, J., 2002. Assessment of vegetation regeneration after fire through multitemporal analysis of AVIRIS images in the Santa Monica Mountains. *Remote Sens. Environ.* 79, 60–71.
- Roberts, D.A., Ustin, S.L., Ogunjemiyo, S., Greenberg, J., Dobrowski, Z., Chen, J., Hinckley, T.M., Dobrowski, S.Z., 2004. Spectral and structural measures of northwest forest vegetation at leaf to landscape scales. *Ecosystems* 7, 545–562.
- Roberts, D.A., Dennison, P.E., Roth, K.L., Dudley, K., Hulley, G., 2015. Relationships between dominant plant species, fractional cover and Land Surface Temperature in a Mediterranean ecosystem. *Remote Sens. Environ.* 167, 152–167. <https://doi.org/10.1016/j.rse.2015.01.026>.
- Roth, K.L., Dennison, P.E., Roberts, D.A., 2012. Comparing endmember selection techniques for accurate mapping of plant species and land cover using imaging spectrometer data. *Remote Sens. Environ.* 127, 139–152. <https://doi.org/10.1016/j.rse.2012.08.030>.
- Roth, K.L., Roberts, D.A., Dennison, P.E., Alonzo, M., Peterson, S.H., Beland, M., 2015a. Differentiating plant species within and across diverse ecosystems with imaging spectroscopy. *Remote Sens. Environ.* 167, 135–151. <https://doi.org/10.1016/j.rse.2015.05.007>.
- Roth, K.L., Roberts, D.A., Dennison, P.E., Peterson, S.H., Alonzo, M., 2015b. The impact of spatial resolution on the classification of plant species and functional types within imaging spectrometer data. *Remote Sens. Environ.* 171, 45–57. <https://doi.org/10.1016/j.rse.2015.10.004>.
- Schaaf, A.N., Dennison, P.E., Fryer, G.K., Roth, K.L., Roberts, D.A., 2011. Mapping plant functional types at multiple spatial resolutions using imaging spectrometer data. *GIScience Remote Sens.* 48, 324–344. <https://doi.org/10.2747/1548-1603.48.3.324>.
- Somers, B., Asner, G.P., 2012. Hyperspectral time series analysis of native and invasive species in Hawaiian rainforests. *Remote Sens.* 4, 2510–2529. <https://doi.org/10.3390/rs4092510>.
- Somers, B., Asner, G.P., 2013. Invasive species mapping in Hawaiian rainforests using multi-temporal Hyperion spaceborne imaging spectroscopy. *IEEE J. Sel. Top. Appl. Earth Obs. Remote Sens.* 6, 351–359. <https://doi.org/10.1109/JSTARS.2012.2203796>.
- Stoffler, T., Kaufmann, C., Hofer, S., Förster, K.P., Schreier, G., Mueller, a, Eckardt, a, Bach, H., Penné, B., Benz, U., Haydn, R., 2007. The EnMAP hyperspectral imager—an advanced optical payload for future applications in Earth observation programmes. *Acta Astronaut.* 61, 115–120. <https://doi.org/10.1016/j.actaastro.2007.01.033>.
- Swain, D.L., Tsang, M., Haugen, M., Singh, D., Charland, A., Rajaratnam, B., Diffenbaugh, N.S., 2014. The extraordinary California drought of 2013/2014: character, context, and the role of climate change. *Am. Meteorol. Soc.* 95, S3–S7.
- Tane, Z., Roberts, D., Koltunov, A., Sweeney, S., Ramirez, C., 2018a. A framework for detecting conifer mortality across an ecoregion using high spatial resolution space-borne imaging spectroscopy. *Remote Sens. Environ.* 209, 195–210. <https://doi.org/10.1016/j.rse.2018.02.073>.
- Tane, Z., Roberts, D., Veraverbeke, S., Casas, Á., Ramirez, C., Ustin, S., 2018b. Evaluating endmember and band selection techniques for multiple endmember spectral mixture analysis using post-fire imaging spectroscopy. *Remote Sens.* 10, 389. <https://doi.org/10.3390/rs10030389>.
- Thompson, D.R., Gao, B.-C., Green, R.O., Roberts, D.A., Dennison, P.E., Lundein, S.R., 2015. Atmospheric correction for global mapping spectroscopy: ATREM advances for the HypPIRI preparatory campaign. *Remote Sens. Environ.* 167, 64–77. <https://doi.org/10.1016/j.rse.2015.02.010>.
- Underwood, E., Ustin, S.L., DiPietro, D., 2003. Mapping nonnative plants using hyperspectral imagery. *Remote Sens. Environ.* 86, 150–161. [https://doi.org/10.1016/S0034-4257\(03\)00096-8](https://doi.org/10.1016/S0034-4257(03)00096-8).
- Ustin, S.L., Roberts, D.A., Pinzo, J., Jacquemoud, S., Gardner, M., Scheer, G., Castan, C.M., 1998. Estimating canopy water content of chaparral shrubs using optical methods. *Remote Sens. Environ.* 65.
- Ustin, S.L., Roberts, D.A., Gamon, J.A., Asner, G.P., Green, R.O., 2004. Using Imaging Spectroscopy to Study Ecosystem Processes and Properties. *BioScience* 54 (6), 523–534. Retrieved from. <http://www.jstor.org/stable/3333946>.
- Verma, M., Tan, B., Friedl, M.A., Ganguly, S., Zhang, X., 2010. Land surface phenology from MODIS: characterization of the Collection 5 global land cover dynamics product. *Remote Sens. Environ.* 114, 1805–1816. <https://doi.org/10.1016/j.rse.2010.04.005>.
- Vina, A., Gitelson, A.A., Rundquist, D.C., Keydan, G., Leavitt, B., Schepers, J., 2004. Monitoring maize (*Zea mays* L.) phenology with remote sensing. *Agron. J.* 96, 1139–1147. <https://doi.org/10.1016/j.jenvman.2011.10.007>.
- Walther, G., Post, E., Convey, P., Menzel, A., Parmesan, C., Beebee, T.J.C., Fromentin, J., Hoegh-guldberg, O., Bairlein, F., 2002. Ecological responses to recent climate change. *Nature* 416, 389–395.
- Wang, D., Liang, S., He, T., Shi, Q., 2015. Estimating clear-sky all-wave net radiation from combined visible and shortwave infrared (VSWIR) and thermal infrared (TIR) remote sensing data. *Remote Sens. Environ.* 167, 31–39. <https://doi.org/10.1016/j.rse.2015.03.022>.
- Wetherley, E.B., Roberts, D.A., McFadden, J., 2017. Mapping spectrally similar urban materials at sub-pixel scales. *Remote Sens. Environ.* 195, 170–183. <https://doi.org/10.1016/j.rse.2017.04.013>.
- Wetherley, E.B., McFadden, J.P., Roberts, D.A., 2018. Megacity-scale analysis of urban vegetation temperatures. *Remote Sens. Environ.* 213, 1–62. <https://doi.org/10.1016/j.rse.2018.04.051>.
- Zhang, X., Friedl, M.A., Schaaf, C.B., Strahler, A.H., Hodges, J.C.F., Gao, F., Reed, B.C., Huete, A., 2003. Monitoring vegetation phenology using MODIS. *Remote Sens. Environ.* 84, 471–475. [https://doi.org/10.1016/S0034-4257\(02\)00135-9](https://doi.org/10.1016/S0034-4257(02)00135-9).
- Zhang, X., Friedl, M.A., Schaaf, C.B., 2006. Global vegetation phenology from Moderate Resolution Imaging Spectroradiometer (MODIS): evaluation of global patterns and comparison with in situ measurements. *J. Geophys. Res. Biogeosci.* 111, 1–14. <https://doi.org/10.1029/2006JG000217>.
- Zomer, R.J., Trabucco, A., Ustin, S.L., 2009. Building spectral libraries for wetlands land cover classification and hyperspectral remote sensing. *J. Environ. Manag.* 90, 2170–2177. <https://doi.org/10.1016/j.jenvman.2007.06.028>.